

## INTRODUCTION

Renal failure is characterized by sudden loss of the ability of the kidneys to excrete wastes, concentrate urine, conserve electrolytes, and maintain fluid balance. <sup>(1)</sup>

It is a frequent clinical problem, particularly in the intensive care unit, where it is associated with a mortality of between 50% and 80% whether occurred acute or chronic onset. <sup>(2)</sup> More recent prospective studies report an overall incidence of acute renal failure of almost 500 per million per year<sup>(3,4)</sup> and an incidence of acute renal failure (ARF) needing dialysis of more than 200 per million per year.<sup>(5)</sup>

Renal failure (also called kidney failure or renal insufficiency) is a medical condition in which the kidneys fail to adequately filter waste products from the blood.<sup>(6)</sup> The two main forms are acute kidney injury, which is often reversible with adequate treatment, and chronic kidney disease, which is often not reversible. In both cases, there is usually an underlying cause.

Acute kidney injury (AKI), previously called ARF,<sup>(7,8)</sup> is a rapidly progressive loss of renal function,<sup>(9)</sup> generally characterized by oliguria (decreased urine production, quantified as less than 400 mL per day in adults,<sup>(10)</sup> less than 0.5 mL/kg/h in children or less than 1 mL/kg/h in infants); and fluid and electrolyte imbalance.

### Definition

Introduced by the Acute Kidney Injury Network (AKIN), specific criteria exist for the diagnosis of AKI:<sup>(11)</sup>

AKI is defined as any of the following (not graded):

- Increase in serum creatinine (SCr) by  $\geq 0.3$ mg/dl within 48 hours or
- Increase in SCr by  $\geq 1.5$  times baseline which is known or presumed to have occurred within the prior 7 days or
- Urine volume  $< 0.5$  ml/kg/hr for 6 hours

### Causes

The causes of acute kidney injury are commonly categorized into pre-renal, intrinsic, and post-renal (pre-renal causes; 40-70% of cases), direct renal parenchymal damage (intrinsic renal causes; 10-50% of cases) and obstructed urine flow (post-renal or obstructive causes; 10% of cases).<sup>(12,13)</sup>

### Pre-renal

Pre renal causes of AKI "pre-renal azotemia" are those that decrease effective blood flow to the kidney. These include systemic causes, such as low blood volume, low blood pressure, and heart failure, as well as local changes to the blood vessels supplying the kidney. The latter include renal artery stenosis, which is a narrowing of the renal artery that

supplies the kidney and renal vein thrombosis, which is the formation of a blood clot in the renal vein that drains blood from the kidney.

These causes stem from the inadequate cardiac output and hypovolemia or vascular diseases causing reduced perfusion of both kidneys. Both kidneys need to be affected as one kidney is still more than adequate for normal kidney function.<sup>(12,13)</sup>

### Intrinsic

Sources of damage to the kidney itself are dubbed intrinsic. Intrinsic AKI can be due to damage to the glomeruli, renal tubules, or interstitium. Common causes of each are glomerulonephritis, acute tubular necrosis (ATN) and acute interstitial nephritis (AIN).<sup>(14)</sup> Intrinsic acute renal failure is often multifactorial; in intensive care the most common cause is sepsis, often accompanied by multi-organ failure.<sup>(15)</sup> Postoperative acute tubular necrosis accounts for up to 25% of cases of hospital acquired acute renal failure, mostly resulting from pre renal causes.<sup>(16)</sup> The third most common cause of hospital acquired acute renal failure is acute radiocontrast nephropathy.<sup>(17)</sup>

### Post-renal

Post-renal AKI is a consequence of urinary tract obstruction. This may be related to benign prostatic hyperplasia, kidney stones, obstructed urinary catheter, bladder stone, bladder, ureteral or renal malignancy. It is useful to perform a bladder scan or a post void residual to rule out urinary retention. In post void residual, a catheter is inserted immediately after urinating to measure fluid still in the bladder (50-100ml) suggests neurogenic bladder. A renal ultrasound will demonstrate hydronephrosis if present.<sup>(18)</sup>

### Diagnosis

The deterioration of renal function may be discovered by a measured decrease in urine output. Often, it is diagnosed on the basis of blood tests for substances normally eliminated by the kidney: urea and creatinine. Both tests have their disadvantages, for instance it takes about 24 hours for the creatinine level to rise, even if both kidneys have ceased to function. A number of alternative markers has been proposed such as neutrophil gelatinase-associated lipocalin (NGAL), Kidney Injury Molecule-1(KIM-1), Interleukin-18 (IL18) and cystatin C, but none are currently established enough to replace creatinine as a marker of renal function.<sup>(19)</sup> However the cause of AKI (pre-renal, renal, post-renal) always easily diagnosed by classic laboratory findings Table (1)

**Table (1): Classic laboratory findings in AKI**<sup>(12,13)</sup>

Classic laboratory findings in AKI				
Type	UOsm	UNa	FeNa	BUN/Cr
Prerenal	>500	<10	<1%	>20
Intrinsic	<350	>20	>2%	<15
Postrenal	<350	>40	>4%	>15

UOsm: urine osmolality

UNa: urine Na level

## Introduction

FeNa: fractional excretion of Na  
BUN: Blood urea nitrogen  
BUN/Cr ratio.

Guidelines for urinary indices whereby established ARF can be distinguished from renal vasoconstriction with intact tubular function, i.e., prerenal azotemia.<sup>(20,21)</sup> Table (2)

**Table (2): Guidelines for urinary indices whereby established ARF can be distinguished from renal vasoconstriction with intact tubular function (pre renal azotemia)**<sup>(20,21)</sup>

Laboratory test	Prerenal azotemia	ARF
Urine osmolality (mOsm/kg)	>500	<400
Urine sodium level (mEq/l)	<20	>40
Urine/plasma creatinine ratio	>40	<20
Fractional excretion of sodium (%)	<1	>2
Fractional excretion of urea (%)	<35	>35
Urinary sediment	Normal; occasional hyaline or fine granular casts	Renal tubular epithelial cells; granular and muddy brown casts

Osm, osmole; Eq, equivalent.

Chronic Kidney Disease (CKD) has numerous causes. The most common causes of CKD are diabetes mellitus and long-term uncontrolled hypertension.<sup>(22)</sup> Polycystic kidney disease is another well-known cause of CKD. The majority of people afflicted with polycystic kidney disease have a family history of the disease. Overuse of common drugs such as aspirin, ibuprofen, and acetaminophen (paracetamol) can also cause chronic kidney damage.<sup>(23)</sup>

Acute kidney injuries can be present on top of chronic kidney disease, a condition called acute-on-chronic renal failure (AoCRF). The acute part of AoCRF may be reversible, and the goal of treatment as with AKI is to return the patient to baseline renal function typically measured by serum creatinine. Like AKI, AoCRF can be difficult to distinguish from chronic kidney disease if the patient has not been monitored by a physician and no baseline blood work is available for comparison.

## Staging

Two similar definitions based on SCr and urine output (RIFLE & AKIN) have been proposed and validated.

- 1- **The RIFLE criteria**, proposed by the Acute Dialysis Quality Initiative (ADQI) group, aid in the staging of patients with AKI.<sup>(17,24)</sup> Table (3)

- **Risk:** Glomerular filtration rate (GFR) decrease >25%, serum creatinine increased 1.5 times or urine production of <0.5 ml/kg/hr for 6 hours.
- **Injury:** GFR decrease >50%, doubling of creatinine or urine production <0.5 ml/kg/hr for 12 hours.
- **Failure:** GFR decrease >75%, tripling of creatinine or creatinine >4 mg/dl (>355 µmol/l) with acute rise >0.5 mg/dl (>44 µmol/l) or urine output below 0.3 ml/kg/hr for 24 hours or anuria for 12 hours.
- **Loss:** persistent AKI or complete loss of kidney function for more than 4 weeks.
- **End-stage renal disease:** need for renal replacement therapy (RRT) for more than 3 months.

**2- AKIN criteria:**<sup>(25)</sup>

**Stage 1:** Increase of SCr more than or equal to 0.3 mg/dl ( $\geq 26.5$  mmol/l) or increase to more than or equal to 150% to 200% (1.5- to 2-fold) from baseline, urine output Less than 0.5 ml/kg/h for more than 6 hours.

**Stage 2:** Increased SCr to more than 200% to 300% (2- to 3-fold) from baseline, urine output Less than 0.5 ml/kg per hour for more than 12 hours.

**Stage 3:** Increased SCr to more than 300% (>3-fold) from baseline, or more than or equal to 4.0 mg/dl (>354 µmol/l) with an acute increase of at least 0.5 mg/dl (44 µmol/l) or on RRT, urine output Less than 0.3 ml/kg/h for 24 hours or anuria for 12 hours.

**Table (3): Comparison of RIFLE and AKIN criteria for diagnosis and classification of AKI** <sup>(17,24,25)</sup>

AKI staging		RIFLE	
Serum creatinine	Urine output (common to both)	Class	Serum creatinine or GFR
<b>Stage 1</b> Increase of more than or equal to 0.3 mg/dl ( $\geq 26.5$ µmol/l) or increase to more than or equal to 150% to 200% (1.5- to 2-fold) from baseline	Less than 0.5 ml/kg/h for more than 6 hours	<b>Risk</b>	Increase in serum creatinine $\times 1.5$ or GFR decrease >25%
<b>Stage 2</b> Increased to more than 200% to 300% (> 2- to 3-fold) from baseline	Less than 0.5 ml/kg per hour for more than 12 hours	<b>Injury</b>	Serum creatinine $\times 2$ or GFR decreased >50%
<b>Stage 3</b> Increased to more than 300% (> 3-fold) from baseline, or more than or equal to 4.0 mg/dl ( $\geq 354$ µmol/l) with an acute increase of at least 0.5 mg/dl (44 µmol/l) or on RRT	Less than 0.3 ml/kg/h for 24 hours or anuria for 12 hours	<b>Failure</b>	Serum creatinine $\times 3$ , or serum creatinine >4 mg/dl (>354 µmol/l) with an acute rise >0.5 mg/dl (>44 µmol/l) or GFR decreased >75%
		<b>Loss</b>	Persistent acute renal failure=complete loss of kidney function >4 weeks
		<b>End-stage kidney disease</b>	ESRD >3 months

The symptoms of acute kidney injury result from the various disturbances of kidney function that are associated with the disease. Accumulation of urea and other nitrogen-containing substances in the bloodstream lead to a number of symptoms, such as fatigue, loss of appetite, headache, nausea and vomiting.<sup>(26)</sup> Marked increases in the potassium

level can lead to irregularities in the heartbeat, which can be severe and life-threatening.<sup>(27)</sup> Fluid balance is frequently affected, though hypertension is rare.<sup>(28)</sup>

Pain in the flanks may be encountered in some conditions (such as thrombosis of the renal blood vessels or inflammation of the kidney); this is the result of stretching of the fibrous tissue capsule surrounding the kidney. If the kidney injury is the result of dehydration, there may be thirst as well as evidence of fluid depletion on physical examination. Physical examination may also provide other clues as to the underlying cause of the kidney problem, such as a rash in interstitial nephritis and a palpable bladder.<sup>(29)</sup>

Inability to excrete sufficient fluid from the body can cause accumulation of fluid in the limbs (peripheral edema) and the lungs (pulmonary edema).<sup>(26)</sup>

A wide variety of pulmonary disorders are associated with renal insufficiency. Pulmonary edema is probably the most common and among the most serious complications of uremia. Pulmonary edema can be defined as an increase in lung fluid caused by extravasation of fluid from the pulmonary vasculature into the interstitium and alveoli of the lungs. The buildup of fluid leads to progressive deterioration of alveolar gas exchange and resulting hypoxia. Pulmonary edema is generally classified as non-cardiogenic (NCPE) and cardiogenic (CPE).<sup>(30,31)</sup>

It is characterized by diffuse alveolar damage, marked increased permeability of the alveolar-capillary membrane, and accumulation of protein-rich fluid in the alveolar air sacs.

## **Pathophysiology**

Under normal conditions, fluid flows from the capillary system to the interstitial space and returns to the systemic circulation through the pulmonary lymphatic system. When capillary fluid efflux into the interstitial space exceeds the lymphatic absorption, pulmonary edema occurs. With cardiogenic pulmonary edema, this is due to increased capillary hydrostatic pressure. In contrast, the major pathophysiologic abnormality causing non-cardiogenic pulmonary edema is increased vascular permeability to proteins, resulting in protein-rich fluid accumulation in the alveolar air sacs.<sup>(32)</sup>

In particular, kidney failure can adversely affect the lungs. This observation dates back to the 1950s when it was identified that patients suffering from AKI manifested abnormal chest X-rays thought to be secondary to 'increased permeability of congested pulmonary capillaries'.<sup>(33)</sup>

Mechanism of pulmonary edema due to AKI: inflammation is a major component of the initiation and exacerbation of AKI. Given that mediators of systemic inflammation are typically activated during AKI and coupled with decrease kidney clearance, such as IL1, uremic toxins, induction of oxidative stress factor as nitric oxide which increase evidence of pulmonary cell apoptosis and increase vascular permeability.<sup>(36,37)</sup> Inflammation and innate immune response are likely important mechanisms connecting the effect of AKI on the lung,<sup>(34,35)</sup> several recent studies have documented lung leukocyte activation and trafficking during experimental AKI<sup>(38,39)</sup> Figure (1)

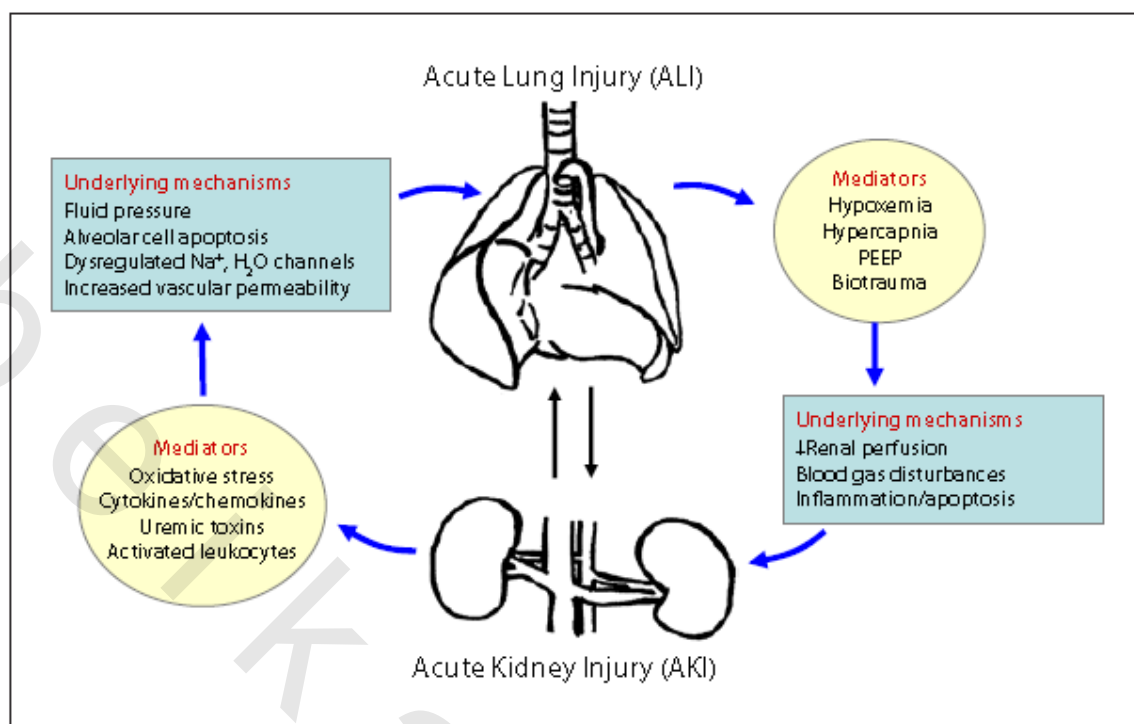


Figure (1): Mechanism of ALI during AKI. <sup>(34-39)</sup>

## Diagnosis of pulmonary edema

### Role of chest radiograph:

Chest radiograph remains the most important method of chest imaging, providing an easily accessible, cheap and effective diagnostic tool. However, it is important to appreciate the limitations and pitfalls of this technique.

Studies have shown that 'routine' daily chest radiographs in critical care are neither beneficial nor cost-effective, and that the chest X-ray (CXR) should be used to answer targeted and specific clinical questions.<sup>(40)</sup>

Basic knowledge of normal thoracic anatomy is essential when interpreting the CXR. A systematic approach to CXR review is necessary to gain the optimum diagnostic information and to avoid potential errors in interpretation.<sup>(41)</sup>

- 1- Airway: large airways, lung, and pleura.
- 2- Bones: clavicles, ribs, and spine.
- 3- Circulation: heart, mediastinum, and vascular Markings.
- 4- Diaphragm.

Radiographic signs that suggest interstitial pulmonary edema include loss of definition of large pulmonary vessels, the appearances of septal lines, interlobar septal thickening, diffuse reticular pattern resembling interstitial fibrosis and peribronchial cuffing seen as bronchial wall thickening as a result of fluid retention in the lung interstitium. Septal lines represent fluid in the deep septae and lymphatics and appear as: Kerley's A lines, which range from 5 to 10 centimeter (cm) in length and extend from the

hilum of the lung toward the periphery in a straight or slightly curved course; and Kerley's B lines, approximately 2cm long, seen in the periphery of the lower lung, extending to the pleura. <sup>(42)</sup> Figure (2) Table (5)

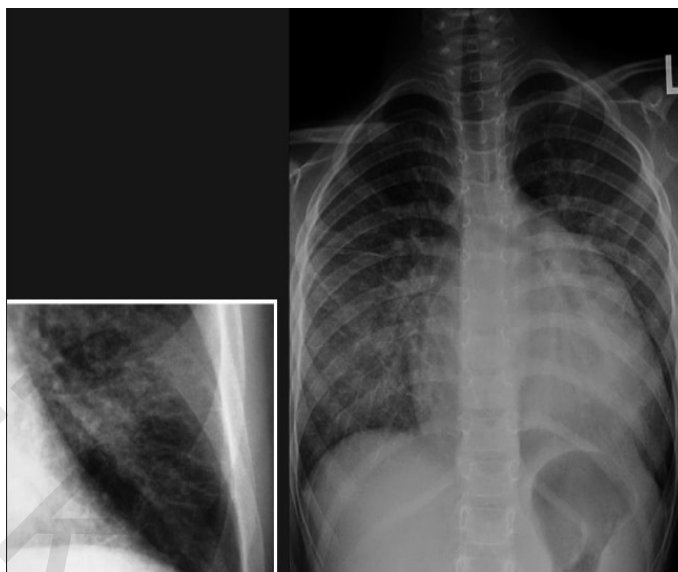


**Figure (2):** Frontal chest radiograph showing features of interstitial pulmonary edema. <sup>(42)</sup>

Differentiation between CPE and NCPE on the basis of radiographic signs alone can be challenging; moreover, the two conditions may coexist. The radiographic features of CPE include cardiomegaly, pleural effusions, upper lobe blood diversion, septal lines, peribronchial cuffing and basal edema. The only exception where the aforementioned changes have not had time to develop is acute myocardial infarction. <sup>(43,44)</sup> Table (4)

**Table (4): Differentiation between CPE and NCPE by CXR** <sup>(43,44)</sup>

<b>Radiographic features</b>	<b>Cardiogenic edema</b>	<b>Non cardiogenic edema</b>
Heart size	Normal or greater than normal	Usually normal
Width of the vascular pedicle	Normal or greater than normal	Usually normal or less than normal
Vascular distribution	Balanced or inverted	Normal or balanced
Distribution of edema	Even or central	Patchy or peripheral
Pleural effusions	Present	Not usually present
Peribronchial cuffing	Present	Not usually present
Septal lines	Present	Not usually present
Air bronchograms	Not usually present	Usually present

Chest X-ray remains by far the best and most used screening test for the detection of pulmonary edema, but it is often difficult to interpret, imprecise and with high interobserver variability <sup>(45)</sup>. The absence of chest X-ray findings does not exclude the presence of a high pulmonary capillary wedge pressure (PCWP).<sup>(46)</sup> There are several explanations for the limited diagnostic accuracy of the chest radiograph. Such as edema may not be visible until the amount of lung water increases by 30 percent. <sup>(47)</sup>

**Table (5): Radiological scoring of Extra vascular lung water (EVLW)<sup>(48,49)</sup>**

Variables	Score*		
Hilar vessels			
Enlarged	1	2	3
Increased in density	2	4	6
Blurred	3	6	9
Kerley lines			
A	4	8	
B	4	8	
C	4	8	
Micronoduli	4	8	
Widening of interlobar fissures	4	8	12
Peribronchial and perivascular cuffs	4	8	12
Extensive perihilar haze	4	8	12
Subpleural effusion	5	10	
Diffuse increase in density	5	10	15

\*The score assigned to each variable depends on the severity of involvement: i.e., Hilar vessels enlarged: 1, normal mild enlargement; 2, moderate enlargement; 3, severe enlargement.

Radiological scoring of EVLW suggest Pulmonary edema if score >15, if score <15 no pulmonary edema.<sup>(48,49)</sup>

Usually, chest x-ray allows adequate recognition of pulmonary edema, with signs evolving as a function of the wedge pressure. At a pulmonary capillary wedge pressure of < 8 mm Hg, the vasculature pattern is normal. As the pulmonary capillary wedge pressure increases to 10-12 mm Hg, the lower-zone vessels appear equal in diameter to or smaller than the upper-zone vessels. At pulmonary capillary wedge pressures of 12-18 mm Hg, the vessel borders become progressively hazier because of increasing extravasation of fluid into the interstitial space. This effect is sometimes evident as Kerley B-lines—horizontal, pleural-based, peripheral linear densities. As pulmonary capillary wedge pressure increases above 18-20 mm Hg, pulmonary edema occurs with interstitial fluid present in sufficient amounts to cause a perihilar “bat wing” appearance. However, full-blown cases of pulmonary edema with high wedge pressure can coexist with a paucity or absence of radiologic signs of pulmonary edema.<sup>(48,50)</sup> Table(6)

**Table (6): Pulmonary venous vessels of patients with pulmonary edema seen using chest x-ray <sup>(48,50)</sup>**

Pulmonary venous vessels distribution	Physiopathology	Estimated pulmonary venous pressure		Value
Normal	None	8-12mmHg		1
Equalization	Pulmonary venous hipertension	13- 15mmHg	Mild	2
			Moderate	3
			Severe	4
Inversion	Pulmonary venous hipertension	16-18mmHg	Mild	5
			Moderate	6
			Severe	7
Perihilar haze	Interstitial edema	> 18mmHg	Mild	+1*
			Moderate	+2*
			Severe	+3*
Subpleural thickening	Interstitial edema	> 18mmHg	Mild	+1*
			Moderate	+2*
			Severe	+3*
Peribronchial cuffing	Interstitial edema	> 18mmHg	Mild	+1*
			Moderate	+2*
			Severe	+3*
Pleural effusion	Interstitial edema	> 18mmHg	Mild	+1*
			Moderate	+2*
			Severe	+3*
Kerley lines	Interstitial edema	> 18mmHg	Mild	+1*
			Moderate	+2*
			Severe	+3*
Consolidation	Alveolar edema	> 25mmHg		11

\* Value added to pulmonary venous vessels distribution grading on the corresponding chest x-ray film.

Another explanation is any radiolucent material that fills the air spaces (such as alveolar hemorrhage, pus, and bronchoalveolar carcinoma) will produce a radiographic image similar to that of pulmonary edema. Technical issues can also reduce the sensitivity and specificity of the chest radiograph, including rotation, inspiration, positive-pressure ventilation, position of the patient, and underpenetration or overpenetration of the film. There is also substantial interobserver variability in the interpretation of radiographs. <sup>(51,52)</sup>

## **Role of chest computed tomography (CT):**

Lung CT is considered as the gold standard for the diagnosis of pneumothorax, pleural effusion, lung consolidation, atelectasis and alveolar interstitial syndrome.<sup>(53-55)</sup>

## **Different types of chest CT scans:<sup>(56)</sup>**

### **1. High-Resolution Chest CT Scan (HRCT):**

HRCT scans provide more than one slice in a single rotation of the x-ray tube. Each slice is very thin and provides a lot of details about the organs and other structures in the patient's chest.

### **2. Spiral Chest CT Scan:**

For this scan, the table moves continuously through the tunnel-like hole as the x-ray tube rotates around the patient. This allows the x-ray beam to follow a spiral path. The machine's computer can process the many slices into a very detailed, three-dimensional (3D) picture of the lungs and other structures in the chest.

### **Advantages:<sup>(57-59)</sup>**

1. CT scanning is painless, noninvasive and accurate.
2. It has the ability to image bone, soft tissue and blood vessels all at the same time and unlike conventional CXR, CT scanning provides very detailed images.
3. CT examination is fast and simple in emergency situations.
4. CT imaging provides real-time imaging, making it a good tool for guiding minimally invasive procedures such as needle biopsies and needle aspirations of many areas of the body, particularly the lungs, abdomen, pelvis and bones.

### **Disadvantages:<sup>(58)</sup>**

1. There is always a slight chance of cancer from excessive exposure to radiation. However, the benefit of an accurate diagnosis far outweighs the risk.
2. It is a costly resource and is not readily available in all hospital contexts.
3. It requires patient transport which, especially in hemodynamically unstable patients, always carries some risk.
4. Pregnant females are relatively contraindicated to have CT scanning.

CT scans should be performed in suspended respiration at total lung capacity. CT has been shown to be superior to plain films in the differentiation of pleural from parenchymal disease.<sup>(60)</sup>

CT scanning is difficult to be used in assessing patients with NCPE and adult respiratory distress syndrome (ARDS), mostly because of problems in transporting and monitoring these severely ill individuals. In addition, CPE can give rise to an appearance similar to NCPE on CT scans. HRCT scanning demonstrates widespread airspace consolidation, which may have predominant distribution in the dependent lung regions. A reticular pattern with a striking anterior distribution is a frequent finding of follow-up CT scanning in ARDS survivors.<sup>(61)</sup>

## **Abnormalities visible on high-resolution CT scans:**

### **1- Ground-Glass Opacity**

Ground-glass opacity, defined as a region of increased lung attenuation not obscuring the underlying vessels, seen in association with interlobular septal thickening or peribronchovascular interstitial thickening. Ground-glass opacity often showed a gravitational predominance, although usually subtle. Some predominance in the parahilar regions was also seen in whereas edema due to increased vascular permeability usually shows a predominant peripheral and sub pleural distribution.<sup>(62)</sup> Figure(3)

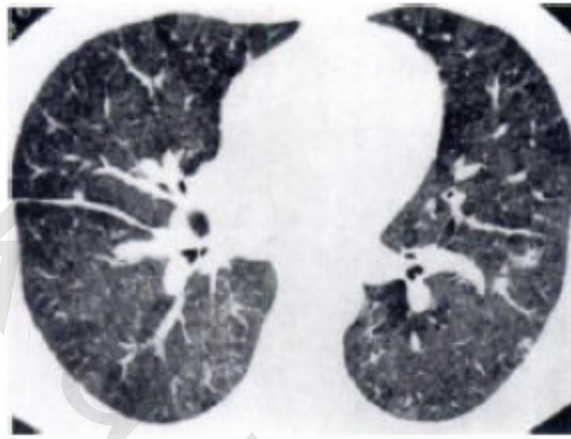


**Figure (3):** HRCT scan through lower lobes prior to treatment. Diffuse ground-glass opacity is visible, with parahilar and posterior predominance. thickening of major fissures can reflect subpleural interstitial thickening or fluid in fissure.<sup>(62)</sup>

### **2- Interlobular Septal Thickening**

Interlobular septal thickening due to pulmonary edema results in linear or reticular opacities 1-5 mm thick, as seen on HRCT scans. These septa are usually thickened by edema fluid accumulating in the interstitium. Septal thickening in patients with pulmonary edema generally appears smooth and uniform, although a focal nodular appearance can reflect the presence of prominent septal veins.<sup>(63)</sup> Figure(4,6)

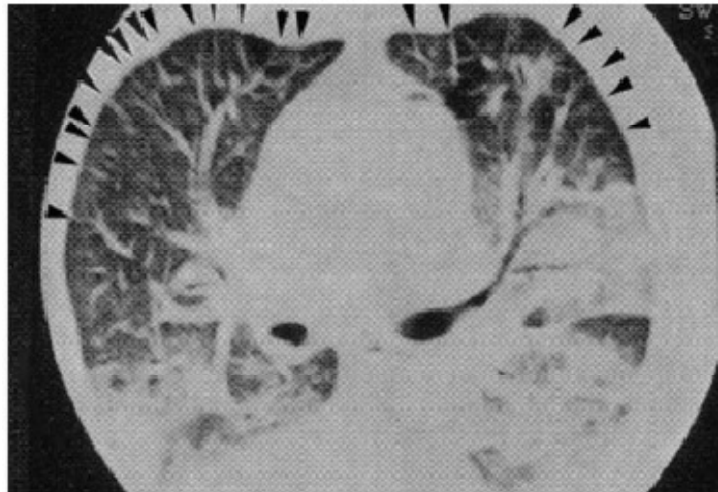


**Figure (4):** CT chest showing acute alveolar and interstitial syndrome. The sub pleural interlobular septa are thickened. <sup>(63)</sup>

### **3- Peribronchovascular Interstitial Thickening**

Peribronchovascular interstitial thickening results in apparent bronchial wall thickening, equivalent to peribronchial cuffing seen on plain radiographs, and can make the central pulmonary vessels or smaller intrapulmonary vessels appear larger than normal. <sup>(63)</sup> Figure(5,6)

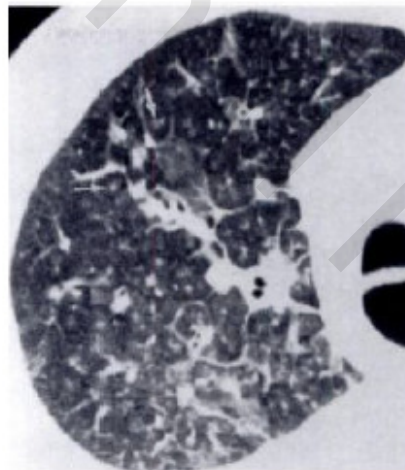


**Figure (5):** High-resolution CT scan through right upper lobe shows ground-glass opacity, which is predominant in dependent lung, ill-defined centrilobular ground-glass nodules (arrows), thickening of interlobular septa, peribronchovascular interstitial thickening, and increased arterial diameter. <sup>(63)</sup>

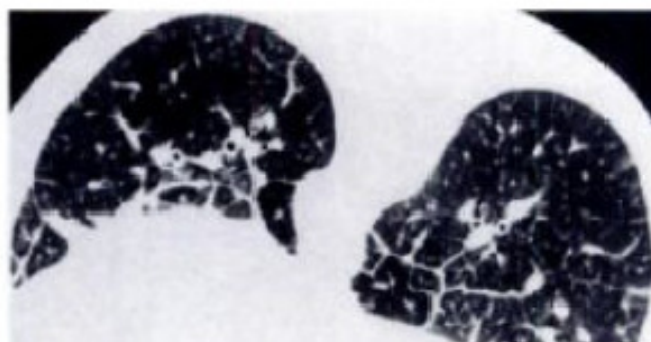


**Figure (6):** Thickened interlobular septa, equivalent to Kerley B lines seen on plain radiographs, are most numerous and of greatest width in dependent lung. These range up to several mm in thickness. Focal nodularity of septa at branching points reflects presence of pulmonary veins. Peribronchovascular interstitial thickening is also evident.<sup>(63)</sup>

#### **4- Increased Vascular Diameter**

In patients with congestive heart failure, pulmonary arteries and veins can be dilated. Dilatation is easiest to recognize in the parahilar regions, where arterial and bronchial diameters can be compared.<sup>(63)</sup>

#### **5- Pleural Abnormalities**

Transudative pleural effusions are a common finding in patients with hydrostatic pulmonary edema, particularly when the edema is severe.<sup>(62)</sup>

### **Role of ultrasound chest**

For many years ultrasound has not been employed for the evaluation of the lung<sup>(64)</sup>. All diagnostic ultrasound methods are based on the principle that ultrasound is reflected by an interface between media with different acoustic impedance. In normal conditions, with aerated lungs, the ultrasound beam finds the lung air and no image is visible, because no acoustic mismatch may reflect the beam, which is rapidly dissipated by air<sup>(65)</sup>. The only detectable structure is the pleura, visualized as a hyperechoic horizontal line, moving synchronously with respiration. When the air content decreases - as in pulmonary edema, pulmonary fibrosis, etc. - the acoustic mismatch needed to reflect the ultrasound beam is created, and some images appear. In the EVLW, the ultrasound beam finds subpleural interlobular septa thickened by edema. The reflection of the beam creates some comet-tail reverberation artifacts, called B-lines or ultrasound lung comets. Figure (7)

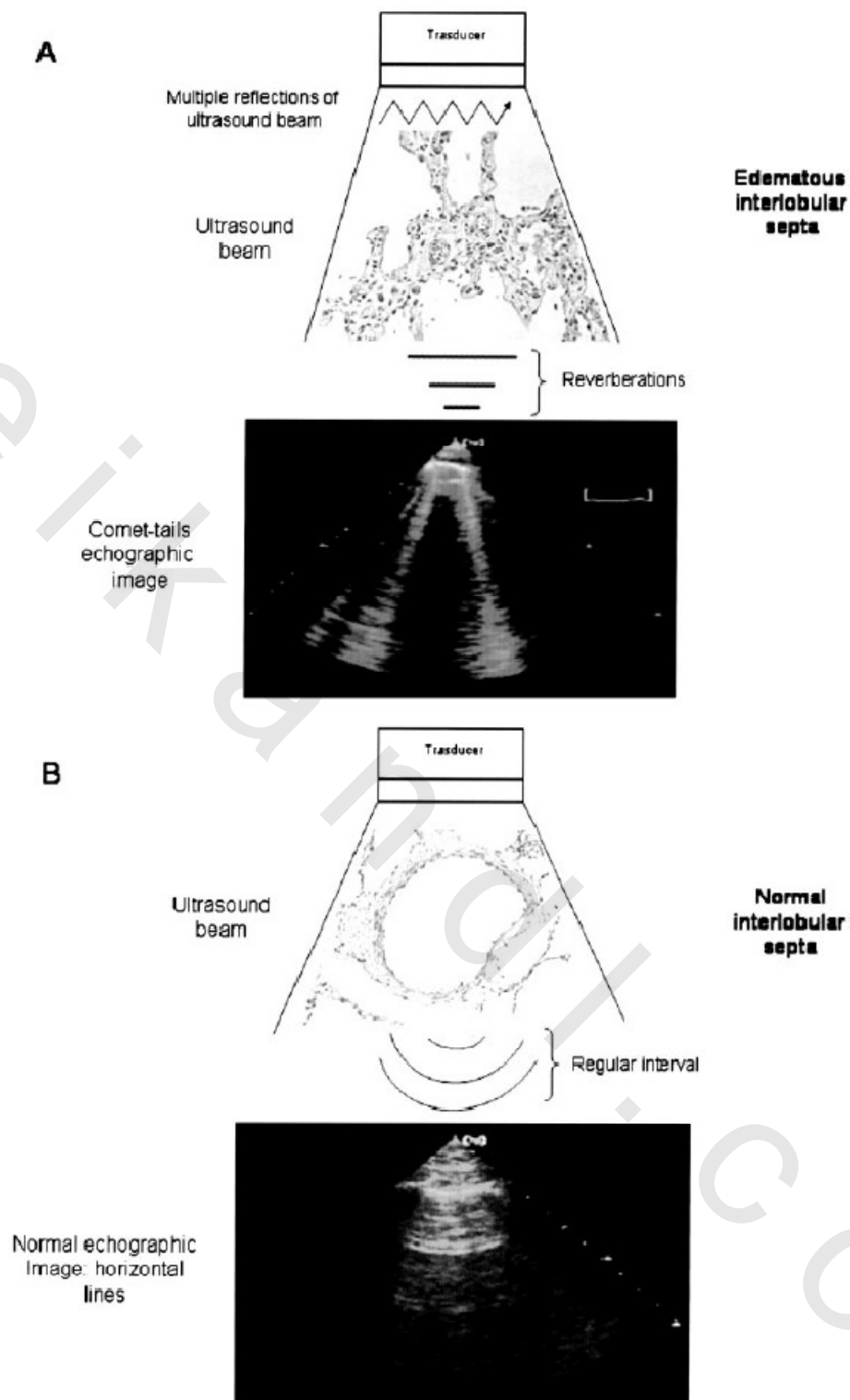


**Figure (7):** Top, A: Typical comet-tail artifacts: hyperechogenic, coherent vertical bundles with narrow basis spreading from the transducer to the further border of the screen. This artifact is composed of multiple microreflections of the ultrasound beam. Bottom, B: Normal subject, with regular, parallel, roughly horizontal hyperechogenic lines due to the lung-wall interface.<sup>(65)</sup>

## The Normal Ultrasound Pattern of the Lung

### The Pleural Line

It is traditionally considered that since the lung is an aerated organ, it cannot be investigated using ultrasound. This assertion should be nuanced. First of all, it is already possible to determine a normal pattern, made up of both static and dynamic signs. Mastering the normal picture should be acquired before any incursion into the pathological domain. A first step will be the recognition of the ribs and their acoustic shadow in a longitudinal scan. Neglecting this step can cause serious mistakes. A hyperechoic, roughly horizontal line is located approximately 0.5 cm below the rib line: the pleural line (Fig. 8). The pleural line reflects the inter-face between the soft tissues (rich in water) of the wall and the lung tissue (rich in air). The pleural line is called the lung-wall interface. The pleural line is distinct from the aponeurotic layers and from the repeated lines in depth, since it is the only structure located 0.5 cm below the rib line (see Fig. 8). A bat can be imagined flying toward us, with the wings as the ribs and the back the pleural line (the bat sign).<sup>(66)</sup>

All lung signs arise at the very level of the pleural line, which represents the parietal pleura in all cases and the visceral pleura in the cases where it is present against the parietal pleura.<sup>(66)</sup>



**Figure (8):** This is the visible pattern when a probe is applied in a longitudinal axis over the thorax of a normal subject. At first sight, only artifacts are shown in this image (air artifacts surrounded by bone artifacts). The superficial layers are visible at the top of the screen. The ribs (vertical arrows) are recognized by their arciform shape with posterior acoustic shadow. Below the rib line (0.5 cm below), this roughly horizontal hyperechoic line (large horizontal arrows) is the pleural line. It indicates the lung surface. The upper rib-pleural line-lower rib profile shapes a sort of bat flying toward us, hence the bat sign, a basic landmark in lung ultrasonography. One can see a deep repetition of the pleural line (small arrows), the A line. This line is located at a precise place, which is the distance between the skin and the pleural line. The pleural line and the A lines are thus precisely located and should not be confused with other horizontal lines located above or below.<sup>(66)</sup>

### **Static Signs**

The static signs are defined by the artifacts arising from the pleural line. They are numerous and their description would have yielded unwieldy labels. For practical purposes, they were given short names using an alphabetic classification.<sup>(66)</sup>

The most clinically relevant artifacts are either roughly horizontal or roughly vertical. The most usual artifact is a roughly horizontal, hyperechoic line, parallel to the pleural line and arising below it, at an interval that is exactly the interval between skin and pleural line. This artifact was called the ultrasound A line (see Fig. 8). As a rule, several A lines are visible at regular intervals. They can be called A1 lines, A2 lines, etc., according to the number of observed lines (their exact number has no clinical relevance, provided there is at least one A line).<sup>(66)</sup>

The second by order of clinical relevance is a comet-tail artifact, roughly vertical, arising from the pleural line, well defined like a laser ray, most often narrow, spreading up to the edge of the screen without fading (i.e., 17 cm on our unit's largest scale), and synchronized with lung sliding (which will be described in Dynamic Signs). This precise artifact has been called the ultrasound B line (Fig. 9, 10). When several B lines are visible in a single scan, the pattern evokes a rocket at lift-off, and we have adopted the term (lung rockets).<sup>(66)</sup>

B-line defined as a echogenic, coherent, dynamic, discrete, laser-like, vertical, hyperechoic image, that arises from the pleural line, extends to the bottom of the screen without fading, and moves synchronously with respiration. Multiple B-lines are the sonographic sign of lung interstitial syndrome, and their number increases along with decreasing air content.<sup>(67)</sup> Figure (9, 10)

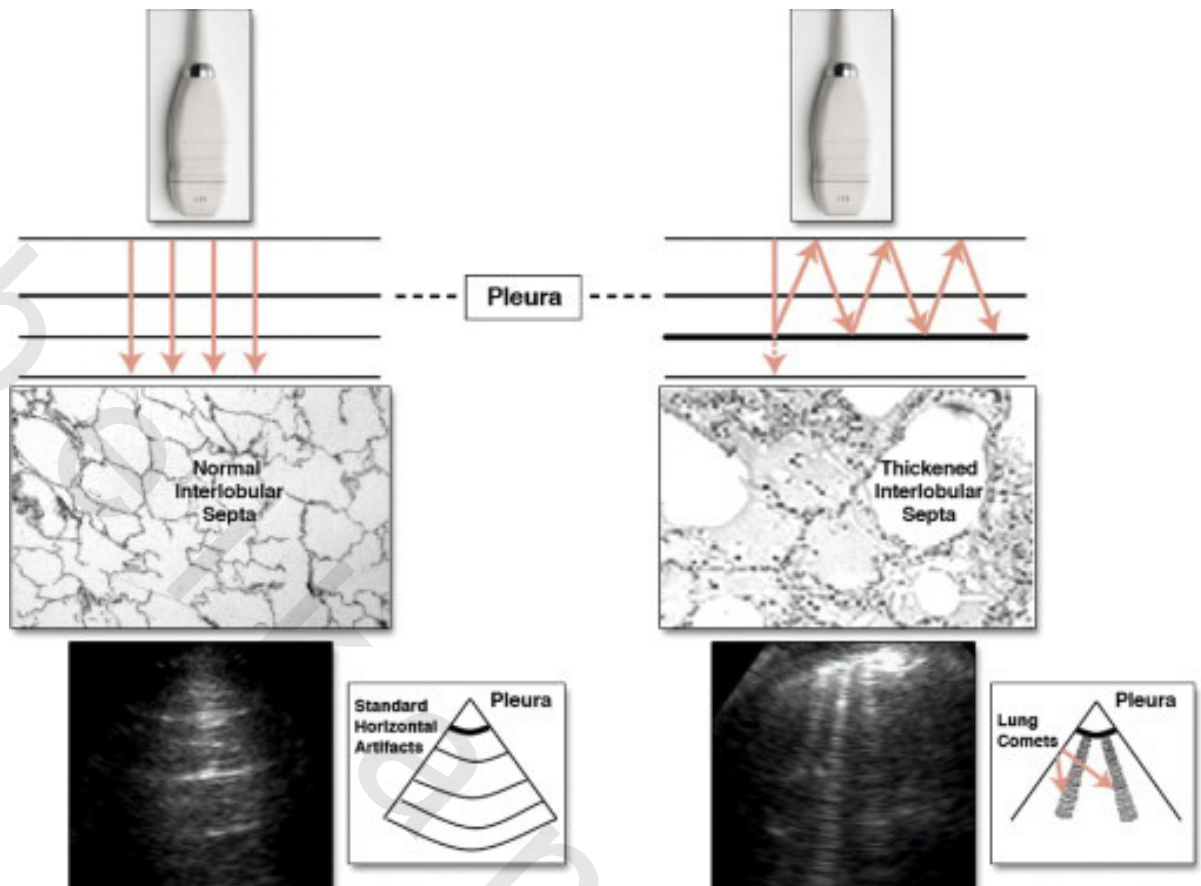


Figure (9): Ultrasound chest in normal person and congested patient. <sup>(67)</sup>

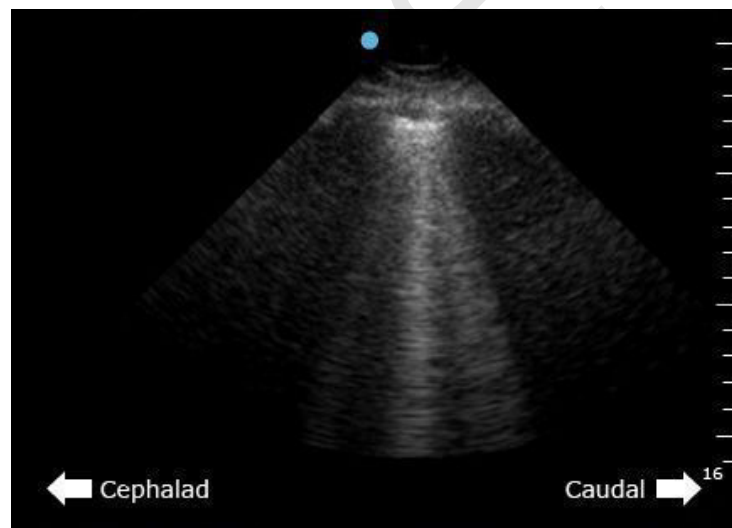


Figure (10): Pleural ultrasound image depicting B lines ("comet tail artifact"). <sup>(67)</sup>

A certain vertical comet-tail artifact should in no case be confounded with a B line. It also arises from the pleural line but is ill defined, not synchronized with lung sliding, and above all, rapidly vanishes, after 1–3 cm (Fig11). This artifact has been called the Z line, the last letter of the alphabet symbolizing the place this artifact should take, since it has no known clinical use. One must describe another critical difference between B and Z lines. B lines erase A lines, whereas Z lines do not. <sup>(67)</sup>



**Figure (11):** Arising from the pleural line, three vertical, ill-defined artifacts, fading after a few centimeters can be defined. These are Z lines, a type of air artifact that should in no case be confused with B lines. <sup>(67)</sup>

Another kind of vertical artifact should be opposed to B lines. This artifact, again a comet-tail, is well defined and spreads up to the edge of the screen without fading. However, this artifact does not arise from the pleural line but from superficial layers, and results in erasing the pleural line. The bat sign is no longer visible. This artifact has been called the E line, E for emphysema (see Fig. 12).

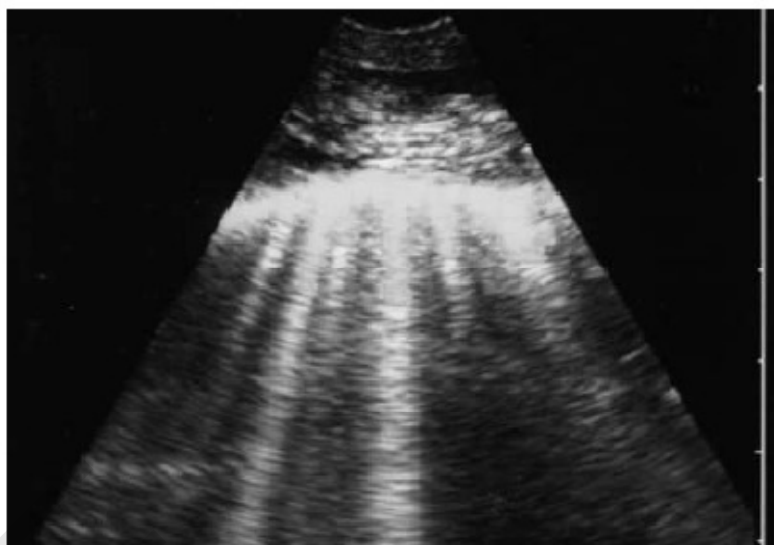


**Figure (12):** In this longitudinal scan of the chest wall in a traumatized patient with clinical parietal emphysema, well-defined comet-tail artifacts are visible, spreading up to the edge of the screen. They may give the illusion of lung rockets, as in Fig. 10, thus ruling out pneumothorax. However, no rib is identified (i.e., the bat sign is absent). The discontinued hyper echogenic line from which the comet tails arise is not the pleural line. Layer of parietal emphysema in a patient with massive pneumothorax.<sup>(67)</sup>

We will see that parietal emphysema (or sometimes parietal shotgun pellets) can generate this artifact, which can mislead the young operator. In some cases, no horizontal or vertical artifact is visible arising from the pleural line, and this pattern is called the O line (or the non-A non-B line). The meaning of O lines is under investigation. For the time being, they should be considered as A lines. C lines are curvilinear, superficial images. Other types of artifacts exist (I, S, V, W and X lines).<sup>(66)</sup>

**- Dynamic Signs:**

The basic dynamic sign is Lung sliding.

**Description:**

Lung sliding shows the sliding of the visceral pleura against the parietal pleura. Careful observation of the pleural line shows a twinkling at this level, in rhythm with respiration. In order to objectify lung sliding, we used the time-motion mode (TM mode). The characteristic pattern obtained, which recalls a beach, can be called the seashore sign (Figure 13). The TM mode provides a definite document, whereas a single frozen image cannot indicate whether lung sliding is present. When lung rockets are associated with lung sliding, a very frequent pattern, they behave like a pendulum that amplifies lung sliding and facilitates its perception. Only a few seconds are sufficient to recognize lung sliding, a crucial advantage.<sup>(68)</sup>

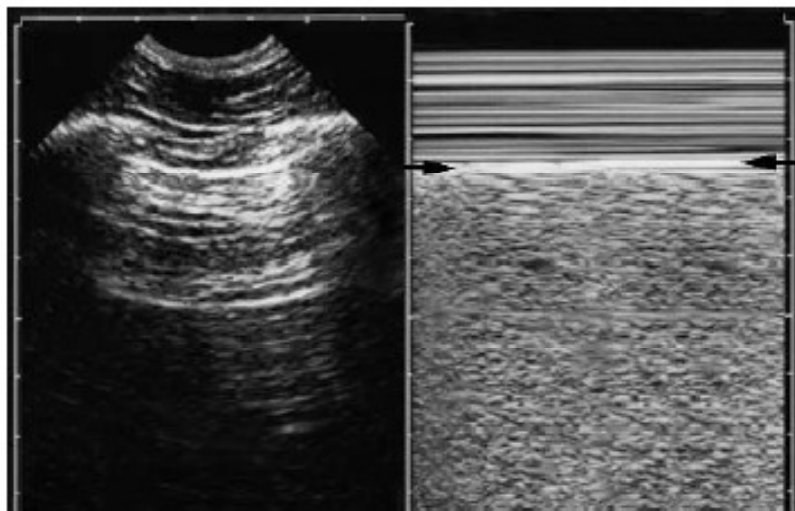


**Figure (13):** The sea shore sign; the left image is static and lung sliding cannot be identified. The right image acquired in time-motion mode and has double component separated by pleural line representing the sea shore sign.<sup>(69)</sup>

**Features of Lung Sliding :**<sup>(68)</sup>

1. The amplitude of lung sliding normally increases from the apex to the base.
2. The pleural line is interrupted by the posterior shadow of the ribs. If the probe is applied over the costal cartilages, there is no interruption since cartilage does not stop the ultrasound beam.
3. Lung sliding is present in spontaneous or conventional mechanical ventilation. It is abolished by jet ventilation.
4. Lung sliding is not abolished by a dyspnea itself, but by the cause of dyspnea as pneumothorax, atelectasis or other causes of abolition.
5. Lung sliding is present in patients with emphysema.
6. Lung sliding is abolished by apnea, as well as any disorder impairing lung expansion.

Lung sliding can be hard to detect in the following cases:<sup>(69)</sup>

1. A history of pleurisy. Lung sliding can be abolished.
2. Severe acute asthma. Lung expansion is very diminished.
3. Subcutaneous emphysema. It considerably damages the image.
4. Certain causes of dyspnea with use of accessory respiratory muscles. Use of accessory respiratory muscles gives a sliding, superficial to the pleural line, it is true, but this situation can be misleading at the beginning of operator training.

5. Inappropriate technique, unsuitable ultrasound device, inadequate smoothing.

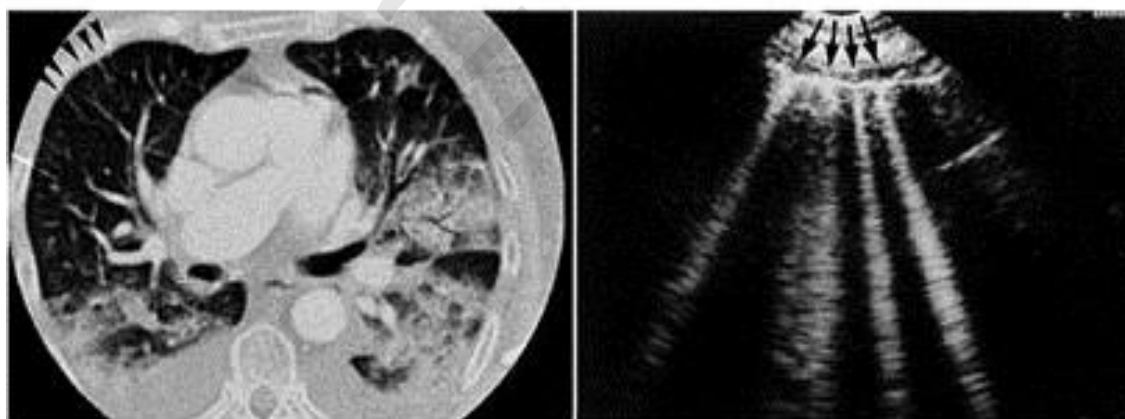
### **Ultrasound signs**

B-line defined as a echogenic, coherent, dynamic, discrete, laser-like, vertical, hyperechoic image, that arises from the pleural line, extends to the bottom of the screen without fading, and moves synchronously with respiration. Multiple B-lines are the sonographic sign of lung interstitial syndrome, and their number increases along with decreasing air content.<sup>(67)</sup> Figure (9, 10)

Eventually, a type of vertical artifact-B-lines-(formerly called comet tails) can be found in normal examination.

There are some anecdotal reports on B-lines since the eighties<sup>(70,71)</sup>. In 1994, Targetta firstly described the presence of B-lines in diseased lungs<sup>(72)</sup>. But it was Daniel Lichtenstein, a French intensivist, who established for the first time the 2 main structural correlates of B-lines, comparing ultrasound findings with chest computed tomography (CT)<sup>(73)</sup>. CT data showed that B-lines were correlated to the thickening of subpleural interlobular septa in pulmonary interstitial edema, and to the fibrotic thickening in pulmonary fibrosis. The modern era of lung ultrasound (LUS) was born. Figure (14)

### **Acute pulmonary edema**



**Chest Computerized  
Tomography**

**Chest Ultrasound**

**Figure (14):** The origin of ULCs from water-thickened interlobular septa. The corresponding CT pattern is shown on the left side.<sup>(73)</sup>

In 2004, Picano and Jambrik, in their laboratory, brought LUS from the Intensive Care Unit to the Cardiology Department, describing the correlation between EVLW assessed by chest X-ray, and the number of B-lines detected by LUS<sup>(74)</sup>. In the following years, experimental<sup>(75,76)</sup>, clinical<sup>(77,78)</sup>, and methodological<sup>(79)</sup> validation of B-lines have been provided. Lung comets represent the US equivalent of Kerley B lines in standard chest X-rays. Figure (15) These artifacts are easily detected with standard US probes.

Remarkably, lung comets are strongly related to LV filling pressure (capillary wedge pressure) and the measurement of LW by US has been formally validated against a golden standard technique such as the indicator thermodilution method in a series of patients submitted to cardiac catheterization.<sup>(80,81)</sup>

**Patient with interstitial edema**

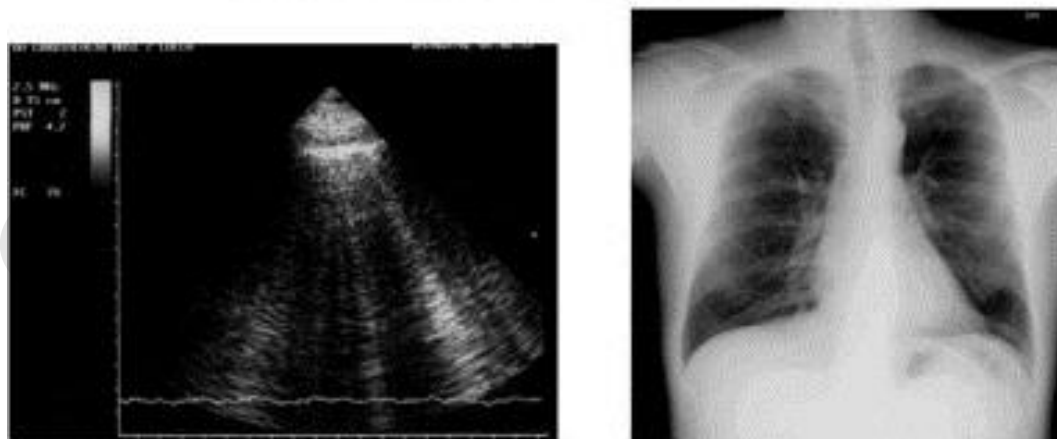


**Figure (15):** Lung comets represent the US equivalent of Kerley B lines in standard chest X-rays.<sup>(74)</sup>

The scanning protocol consists of scanning in the parasternal, mid clavicular, anterior axillary, and mid axillary positions of the second to fifth intercostal spaces on the right side and second to fourth spaces on the left side for a total of 28 positions per complete examination.(Figure 16)<sup>(77)</sup>

Methodology for lung ultrasound evaluation. Thoracic scanning areas for semiquantitative assessment of B-lines (Figure 16)

right side	Mid-axillary	Anterior axillary	Mid-clavicular	Para-sternal	Inter-costal space	Para-sternal	Mid-clavicular	Anterior axillary	Mid-axillary	left side
					II					
				III						
				IV						
				V						

**Figure (16):** B-lines score.<sup>(77)</sup>

The sum of B-lines found on each scanning site yields a score, denoting the extent of extravascular fluid in the lung. In each scanning site, B-lines may be counted from zero to ten. Zero is defined as a complete absence of B-lines in the investigated area; the full white screen in a single scanning site is considered, when using a cardiac probe, as corresponding

to 10 B-lines (figure 17). Sometimes B-lines can be easily enumerated, especially if they are a few; whereas, when they are more numerous, it is less easy to clearly enumerate them, since they tend to be confluent. In this situation, in order to obtain a semiquantification of the sign, one can consider the percentage of the scanning site occupied by B-lines (i.e. the percentage of white screen compared to black screen) and then divide it by ten.<sup>(75)</sup>

B-lines were counted and recorded for each time point on a data collection sheet; their sum yields the overall B-line score (BLS) Lung aeration score. On the basis of this score, we will group patients into 3 categories (mild <14 comets; moderate 14 to 30 comets and severe >30 comets)<sup>(82)</sup>.

**How to enumerate B-lines.**

Each hyperechogenic vertical stripe, spreading from the pleural line and extending to the edge of the screen, is a B-line. When using a cardiac probe, a whole white screen is considered as corresponding to a plateau value of 10 B-lines.

At every scanning site, ultrasound lung comets (ULC) could be counted from 0 to 10. Zero is defined as a complete absence of ULC in the investigated area, while the full white screen is considered, when using a cardiac probe, as corresponding to 10 lung comets. The sum of the comet-tail signs yielded a score denoting the extent of extravascular fluid in the lung.<sup>(82)</sup>

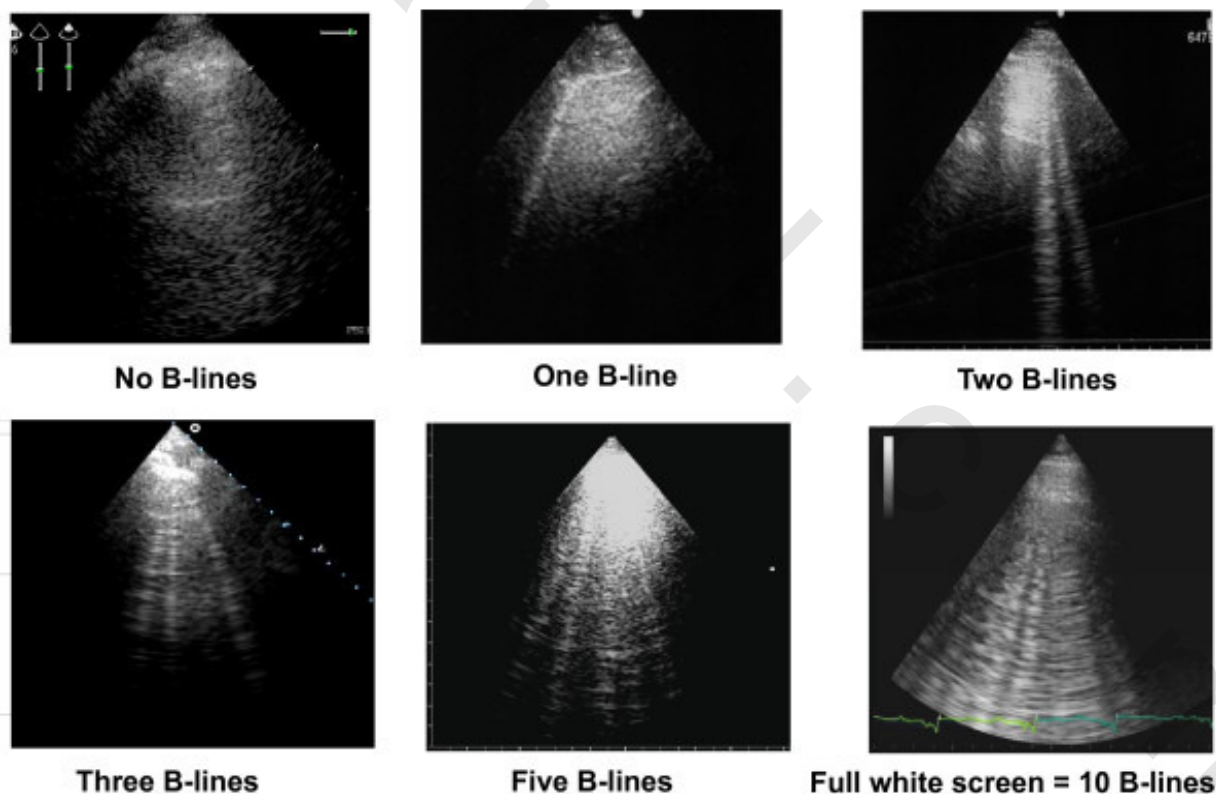


**Figure (17): B-lines counting.**<sup>(75)</sup>

## **Pathological and Nonpathological Locations of Lung Rockets**

- The b lines can be occasionally observed in normal subjects, possibly indicating the small scissura.<sup>(83)</sup>
- Lung rockets localized at the last intercostals space are found in 28% of normal subjects.<sup>(83)</sup>
- Lung rockets located at the lateral wall but including more than two intercostal spaces above the diaphragm should be considered abnormal. The label used is (extensive lateral rockets). In general, more posterior analysis usually shows alveolar changes.<sup>(83)</sup>
- Posterior lung rockets in supine patients are usual, and possibly indicate that the lung water preferentially accumulates in the dependent areas. Analysis of CTs without lung disorders clearly shows these dependent changes. On the other hand, the absence of posterior rockets in a chronically supine patient is singular, and may mean, if validated, substantial hypovolemia.<sup>(83)</sup>

An examination was considered normal when a score of  $\leq 5$  ULCs was defined as a normal echographic chest pattern, as it has been reported that healthy patients may have a small number of ULCs, especially confined laterally to the last intercostal spaces above the diaphragm.<sup>(84)</sup>

Now examination consider normal when presence of fewer than three B-line artifacts in the entire scanned surface.<sup>(65,74)</sup>

### **The following points are highly suggestive of non cardiogenic pulmonary edema**

- Pleural lines abnormalities defined as thickenings greater than 2 mm, evidence of small sub pleural consolidations or coarse appearance of the pleural line.
- Areas with absent or reduced "sliding" sign with respect to adjacent or controlateral zones at the same level on the opposite hemithorax.
- "Spared areas" defined as areas of normal lung pattern in at least one intercostal space surrounded by areas of AIS.
- Consolidations defined as areas of hepatisation (tissue pattern) with presence of air bronchograms.<sup>(85)</sup>
- Pleural effusion defined as anechoic dependent collections limited by the diaphragm and the pleura.<sup>(85)</sup>

"Lung pulse" defined as absence of lung sliding with the perception of heart activity at the pleural line.<sup>(86)</sup>

**Role of echocardiography:**

Bedside transthoracic echocardiography can evaluate myocardial and valvular function and can help identify the cause of pulmonary edema.<sup>(87)</sup>

Although echocardiography is effective in identifying left ventricular systolic dysfunction and valvular dysfunction, it is less sensitive in identifying diastolic dysfunction.<sup>(88)</sup> Thus, a normal echocardiogram by standard methods does not rule out cardiogenic pulmonary edema. Newer echocardiographic techniques such as Doppler tissue imaging (DTI) of the mitral-valve annulus may be used to determine left ventricular end-diastolic pressure and to assess diastolic dysfunction.<sup>(89)</sup>

Diastolic dysfunction is the primary mechanism responsible for dyspnea in patients with PE due to acute renal failure, irrespective of the presence or severity of systolic dysfunction<sup>(90-93)</sup>. Doppler echocardiography has become the noninvasive technique of choice for the evaluation of diastolic function.<sup>(94,95)</sup>

For assessing LV diastolic function, mitral inflow and DTI were also used. The early diastolic velocity (E), the deceleration time from the peak of the early diastolic wave to baseline (E-Dec time), the peak late diastolic mitral inflow (A) and the E/A ratio were assessed. The mitral annular motion velocity (E') was recorded at the mitral annulus site in the apical 4-chamber view by tissue Doppler echocardiography then E/E' were calculated.<sup>(96,97)</sup>

The ratio of peak transmitral early diastolic velocity (E) to peak early diastolic velocity of mitral annular motion (E'), derived from conventional pulsed-wave Doppler echocardiography and DTI, is widely used for non-invasive estimation of LV filling pressure.<sup>(96,97)</sup> (Figure 18,19)

**Mitral inflow velocities examination**

Pulsed wave Doppler (PW-Doppler) allows the measurement of velocities at the level of the sample volume. Two flow velocity envelopes can be seen during diastole in persons with sinus rhythm: the E-wave, representing the early, passive filling of the left ventricle, and the A-wave, that happens late in diastole, representing the active filling, the atrial contraction.<sup>(96,97)</sup> Figure (18)

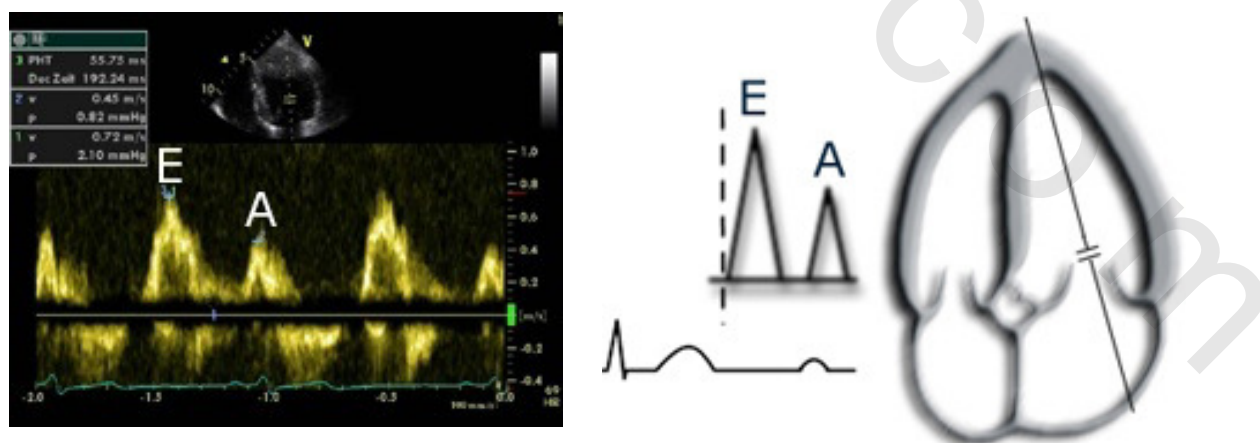


**Figure (18):** Mitral inflow velocities examination.<sup>(96,97)</sup>

**Mitral annular velocities examination**

Slow wall velocities can be assessed with DTI. The sample volume, when placed at the medial mitral annulus, shows slower velocities as when placed at the lateral annulus.<sup>(96,97)</sup> Figure (19)

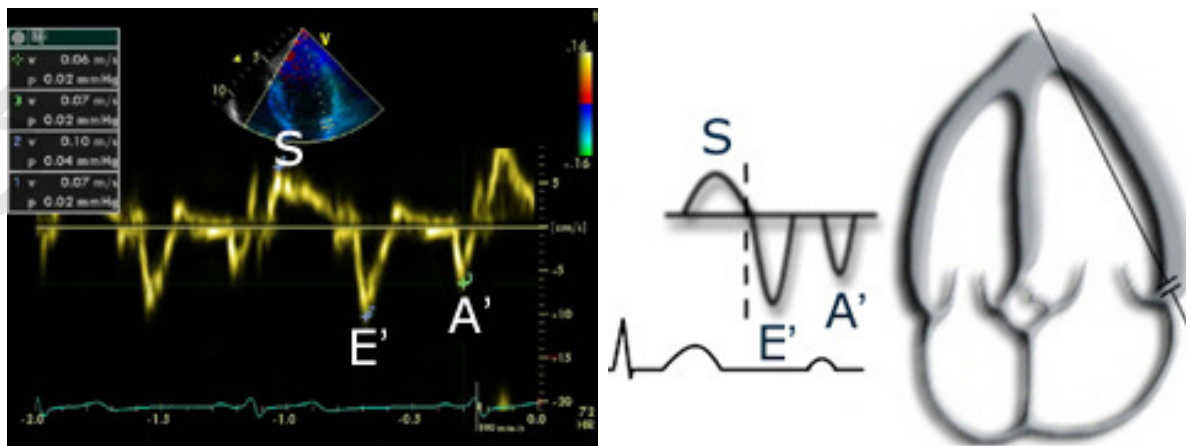


**Figure (19):** Mitral annular velocities examination.<sup>(96,97)</sup>

A new equation enables non-invasive assessment of PCWP, the Nagueh-Formula:  $1,9 + (1,24 \cdot E/E') = PCWP$ , that could make estimation of diastolic function in some way easier, since  $PCWP \approx mLAP \approx LVEDP$ ., to calculate PCWP.<sup>(96)</sup>

DTI is a new ultrasound modality that records systolic and diastolic velocities within the myocardium.<sup>(98-102)</sup> and at the corners of the mitral annulus<sup>(103-105)</sup>. The velocity of annular motion reflects shortening and lengthening of the myocardial fibers along a longitudinal plane. The early diastolic velocity recorded at the lateral corner of the annulus ( $\acute{e}$ ) has been recently demonstrated to decline progressively with age and to be reduced in pathologic LV hypertrophy<sup>(105)</sup>, as well as in patients with restrictive cardiomyopathy<sup>(106)</sup>.

Because septal  $\acute{e}$  is usually lower than lateral  $\acute{e}$  velocity, the  $E/\acute{e}$  ratio using septal signals is usually higher than the ratio derived by lateral  $\acute{e}$ , and different cutoff values should be applied on the basis of LV EF, as well as  $\acute{e}$  location, it is useful to consider the range in which the ratio falls. Using the septal  $E/\acute{e}$  ratio, a ratio  $<8$  is usually associated with normal LV filling pressures, whereas a ratio  $>15$  is associated with increased filling pressures.<sup>(107)</sup> A number of recent studies have noted that in patients with normal EFs, lateral tissue Doppler signals ( $E/\acute{e}$ ) have the best correlations with LV filling pressures and invasive indices of LV stiffness. These studies favor the use of lateral tissue Doppler signals in this population.<sup>(108,109)</sup>

Elevated filling pressures are the main physiologic consequence of diastolic dysfunction.<sup>(90,110)</sup> Filling pressures are considered elevated when the mean pulmonary PCWP is  $>12$  mm Hg or when the LVEDP is  $>16$  mm Hg.<sup>(91)</sup>

Direct measurement of PCWP via catheterization is the gold standard to evaluate hemodynamic congestion, but its invasive nature limits clinical utility.

Transmitral to early diastolic annular velocity ratio ( $E/E'$ ) obtained via DTI correlates strongly with LV filling pressures.<sup>(110)</sup> An  $E/E'$  ratio  $> 10$  identified PCWP  $> 15$  mm Hg with a sensitivity of 92% and a specificity of 80%<sup>(111)</sup>

Increased pulmonary venous congestion has been thought to be caused by increased left ventricular (LV) filling pressure and worsening systolic and diastolic function. Indeed, a nonphysiologic abrupt increase in PCWP can cause ultrastructural changes in the walls of pulmonary capillaries resulting in alveolar edema. It is therefore not surprising that the degree of diastolic dysfunction proved to be the strongest predictor of ULCs. The data corroborate previous findings describing a significant linear correlation between ULC score and  $E/E'$  ratio, a surrogate marker for left sided filling pressures.<sup>(81)</sup>

Haemodialysis provides a unique opportunity to evaluate the effect of a preload reduction on Doppler parameters currently used to assess LV diastolic properties. In this specific setting, recent clinical studies conducted in patients with chronic renal failure have yielded discrepant results. Some studies suggest that mitral annular early diastolic velocity behaves as preload independent index of left ventricular relaxation, however some studies report that it is preload-dependent<sup>(112-115)</sup> and can be decrease significantly after dialysis (Figure 20).

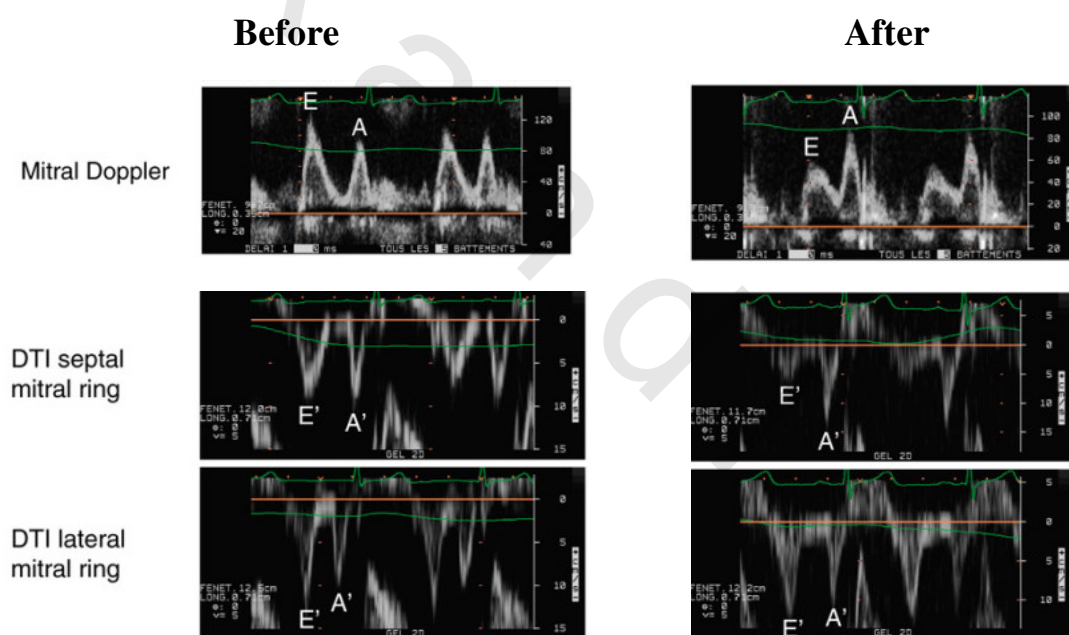


**Figure (20):** DTI mitral valve before and after dialysis.<sup>(112-115)</sup>

The volume of ultrafiltration withdrawn from patients is presumably a major determinant of the sensitivity of Doppler parameters to preload reduction. Accordingly, we sought to evaluate whether the new indices of LV diastolic function provided by DTI of the mitral annulus and colour M-mode were altered by hemodialysis and if could be used as noninvasive modality to assess EVLW.